Invited Paper

MOEMS Pressure Sensors For Propulsion Applications*

Joseph T. Boyd[1], Samhita Dasgupta[1,3], and Howard E. Jackson[2]
1. Department of Electrical and Computer Engineering and Computer Science, University of Cincinnati, Cincinnati, OH 45221-0030
2. Department of Physics, University of Cincinnati, Cincinnati, OH 45221-0011
3. Taitech, Inc., AMC P.O. Box 33630, WPAFB OH 45433-0630

ABSTRACT

Pressure sensors utilizing microelectromechanical systems (MEMS) technology for fabrication of the sensing element, interrogation by fiber optics, and which are suitable for propulsion applications are described. Devices utilizing micro-opto-electro-mechanical systems (MOEMS) technology are often better suited for harsh environments than electrically interrogated MEMS devices, so with sturdy packaging these optical devices may be useful to many propulsion applications. MOEMS pressure sensors can also be incorporated into arrays for detailed spatial characterization along with inherent high speed temporal characterization. Such characterization is expected to be very useful for propulsion systems.

This presentation will first review optical-MEMS pressure sensor configurations. We will then concentrate on configurations most suitable for high speed applications in harsh environments. Examples of experimental results for static pressure tests as well as for dynamic pressure tests carried out in a shock tube demonstrating good linearity, sensitivity and time response will then be presented. Hybrid and monolithic array configurations will be presented. A discussion of the use of wavelength division multiplexing (WDM) for efficient accessing of array elements will also be included.

Keywords: Fiber-optic, micromachined, sensor arrays, dynamic response, Fabry-Perot, pressure sensors.

1. INTRODUCTION

Micro-opto-electro-mechanical systems (MOEMS) technology incorporates many advantages for fabrication of pressure sensors, particularly pressure sensors for propulsion applications. Propulsion applications require a rugged device, a high speed pressure response signal, and a configuration allowing incorporation into an array of pressure sensors. Examples of propulsion applications include:

1. Determination of vibration characteristics of turbine blades for high cycle fatigue determination,
2. Use of pressure readout in the real time control and operation of airborne scramjet systems,
3. Use of fast spatial and temporal response arrays for use as novel instrumentation in wind tunnel testing,
4. Use of sensors in high-temperature, high-vibration environment,
5. Study of aero-mechanical characteristics of turbine systems.

MEMS devices are generally rugged structures. A MEMS device that is interrogated by an optical fiber, thus forming a MOEMS device, can be packaged in such a way to form a rugged overall sensor that can withstand harsh environments. MOEMS sensing elements are characterized by large bandwidth and high sensitivity. Because of the general sensor device configuration and of the use of MEMS fabrication technicques, the formation of arrays is a natural extension of single device fabrication. The use of optical interrogation invites the possibility for interrogation of multiple sensors, such as in an array, by utilizing wavelength division multiplexing (WDM). This would simplify collecting array signals and may be more effective than using electronic interrogation. We thus anticipate that MOEMS pressure sensors will be useful for propulsion applications because their structure can readily be incorporated into arrays, they provide sufficiently good time response, and they have survived harsh environments.

2. MOEMS PRESSURE SENSORS

Optical fiber sensors can have a large variety of configurations [1]. Optical pressure sensors of the type we are considering have been reported in a variety of configurations, including those that utilize light radiating from a fiber and

* This study has been supported in part by a joint AFRL/DAGSI (Dayton Area Graduate Studies Institute) grant, AFOSR, the propulsion directorate of AFRL, and NASA.

In *MOEMS and Miniaturized Systems*, M. Edward Motamedi, Rolf Göring, Editors, Proceedings of SPIE Vol. 4178 (2000) • 0277-786X/00/$15.00

those that utilize optical guided waves to interrogate MEMS structures. Examples of pressure sensors utilizing unguided light for interrogation include those using modulation of the air gap of a Fabry-Perot interferometer by deflection of a diaphragm [2-4], photoelastic modulation of polarization state [5], and interferometric detection of the stress-dependent resonant frequency of an optically excited vibrating beam [6,7] and mechanical coupling of a diaphragm. Previously there has been some work involving optical fiber sensors being utilized to characterize engine and wind tunnel environments [8-10].

Examples of pressure sensors using guided light to interrogate MEMS structures generally involve integration of an interference structure, such as a ring resonator or a Mach-Zehnder interferometer, to interrogate the MEMS structure. In these later structures interrogation is generally accomplished by photoelastic modulation of the interferometer optical path length difference [11-15]. Light from fibers is coupled into and out of these optical waveguide devices. For diaphragm MEMS structures guided wave interrogation generally results in the input and output fiber axes being parallel to the diaphragm surface, in contrast to sensors utilizing unguided light where the fiber axis is generally normal to the diaphragm surface. Guided wave configurations are thus more attractive for applications involving a thin sensor profile.

An example of a guided wave configuration involving a Mach-Zehnder interferometer has been earlier demonstrated by our group. In this sensor a micromachined diaphragm and an unbalanced Mach-Zehnder waveguide interferometer are fabricated on a common silicon substrate, as shown in Fig. 1. The sensitivity to pressure is maximized by positioning one

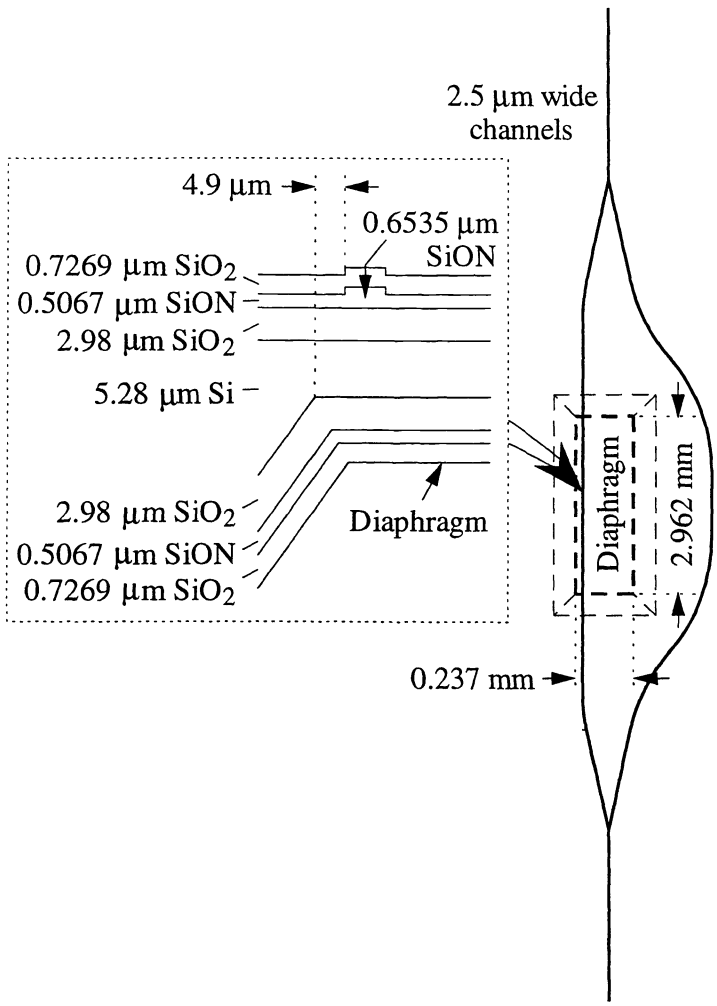

Figure 1. Plan view of Mach-Zehnder interferometer showing diaphragm detail in cross section.

arm of the interferometer (the sensing arm) on top of one of the long edges of the diaphragm while the other arm (the reference arm) is remote from the diaphragm and unstressed. The physical length imbalance of the interferometer arms is 100 μm. A difference in pressure across the diaphragm causes it to deflect, thereby imparting a stress to the waveguide on top of the diaphragm edge. Through the photoelastic effect, this stress alters the refractive index of the waveguide films, thereby altering the effective index of the guided mode, so that the interferometer output intensity is changed and detected. We have demonstrated a sensor of this type with a broadband light source to produce a spectrally encoded measurement [15]. This spectral encoding mechanism is advantageous as it is not readily degraded by transmission through optical fibers. Figure 2 shows a plot of measured phase change as a function of pressure for both TE and TM wave polarizations. The coupling of the photoelastic tensor to the TE polarization is much smaller than for TM, but collecting this information allows effective temperature compensation.

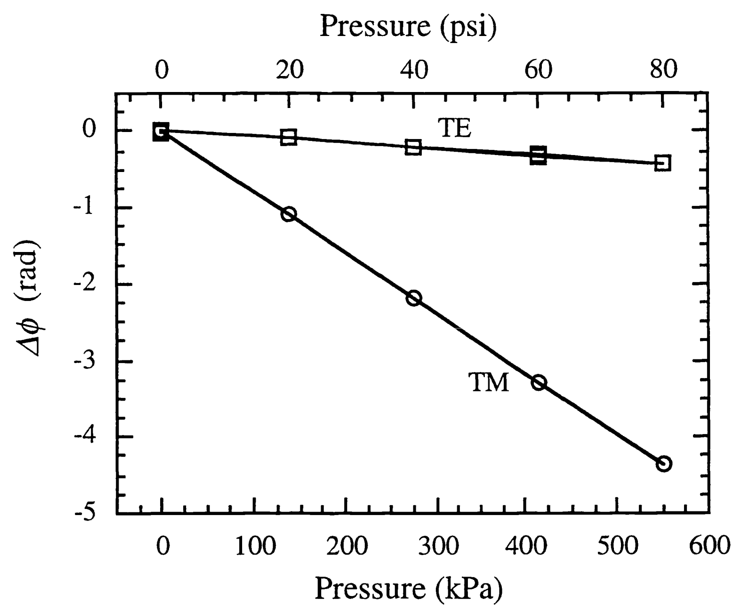

Figure 2. Measured TE and TM phase shifts as functions of pressure at room temperature [15].

An example of a MOEMS pressure sensor using unguided light radiated from an optical fiber to interrogate a MEMS diaphragm is now considered. This structure utilizes reflection of the light from the diaphragm and a second reflecting surface to interrogate the position of the diaphragm and thus the pressure. These two reflectors form an interferometer and the reflection from this interferometer is sensitive to spacing of the two reflectors.As one of the partial reflecting surfaces is a pressure-sensitive diaphragm, changes in external pressure will alter the spacing between reflectors. In our configuration, shown in Fig. 3, the interferometer is formed by two parallel surfaces, one being the Si/air interface and the other the air/glass interface. Details of the design, fabrication, and operation of the structure shown in Fig. 3 appear in a companion paper [17].

A number of these sensors have undergone exstensive static and dynamic testing. Ranges of pressure for which a linear response results can be varied by design and sensor sensitivity is generally several millivolts per psi. Figure 4 shows a sensor response curves for a sensor which had a diameter of 600 μm, a cavity depth of 0.7 μm, and a diaphragm thickness of 30 μm. The sensor shows a monotonic response over a pressure range over 40 psi. The responsivity of this sensor is around 2.7 mV/psi.

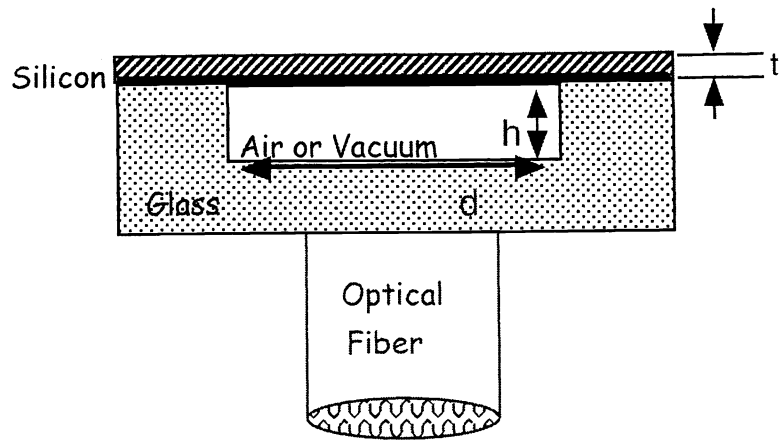

Figure 3. Configuration of the fiber-coupled interferometer MOEMS pressure sensor [16].

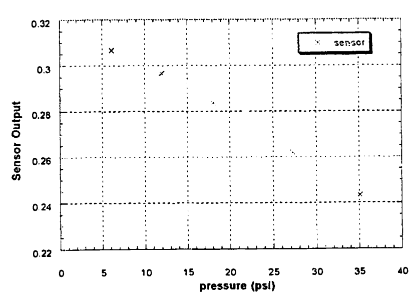

Figure 4. Static response for pressure sensor having a diameter of 600 μm, a cavity depth of 0.7 μm, and a diaphragm thickness of 30 μm.

Figure 5-a shows a typical time trace of the response of the detector due to a shock wave generated in a shock tube facility for the sensor characterized in Fig. 4. A sharp response to the shock wave pressure rise is immediately noticeable. The sensor shows some overshoot before reaching a constant output. The pressure step magnitude is about 10 psi as expected from the theoretical calculation. Fluctuations in the response before and after the shock wave result from noise associated with the shock tube system.

The response of the sensor and the ideal step inputs were weighted with an exponential window to suppress the leakage of frequency spectrum due to taking an incomplete cycle. Figure 5-b shows a plot of the average frequency response. Many traces were individually analyzed, and then averaged in the frequency domain. The plotted line shows the averaged response from multiple samples. A high peak above 100 kHz was apparent in the results. The response of the sensor system, is a combination of the sensor response and the sampled detector-amplifier response, which, for components used in this work, was limited to 210 KHz. Based on this limitation, we infer that the overall response of the sensor is currently limited by the detector response. An encouraging result of these dynamic calibration tests is the usable frequency of the fabricated sensor. The flat response of the sensor extends up to 50 kHz. These response characteristics compare favorably with current and developing sensor technologies.

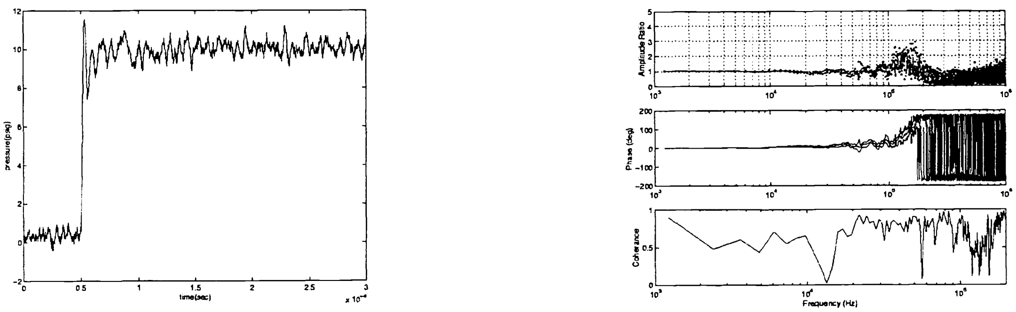

Figure 5. Dynamic response of the fabricated pressure sensor. Figure 5a shows the time response of the sensor signal to the change in pressure. Figure 5b shows the calculated transfer function for the response step. A flat response upto 50 KHz is obtained in this figure along with a peak response above 100 KHz.

3. ARRAY ISSUES

Use of the MOEMS pressure sensors for propulsion applications would greatly benefit from the presence of two-dimensional arrays of sensors that would obtain spatially and temporally resolved data. In order to record pressure maps at sequential instances in time, the data from all the elements in the need to be acquired simultaneously. This suggests that multiplexing techniques may be useful as the array sizes get larger. We are currently trying to resolve issues regarding the fabrication, the packaging and the readout of such arrays.

Fabrication of the arrays requires very tight control of the diaphragm thickness and surface uniformity across the entire array. The etching process is the primary step that affects the above properties of the diaphragm. Our recent results indicate that the etching process, when controlled properly, yields surface quality that is adequate for array fabrication. We are currently in the process of packaging initial arrays for preliminary evaluation.

Packaging of the arrays for propulsion applications is a critical issue. The package has to be sturdy enough to survive the high temperature, high vibration environment and isolate the sensor from the non-essential environmental effects. In addition, the package has to be designed such that the integrity of the sensor remains intact over an extended period of time. The arrays that are currently being packaged are linear arrays consisting of six sensors. For this initial testing phase, the sensors are each connected to a separate fiber so that all six sensors may be read simultaneously. These initial tests will provide information on the response uniformity of the sensors, the packaging needs and/or pitfalls and the level of resolution required for particular applications. Large two-dimensional arrays using separate fibers for each sensor are impractical and hence, multiplexed hybrid and monolithic arrays are being currently considered.

The hybrid arrays currently being considered will be constructed using fiber Bragg gratings that are placed onto V-grooves etched in a silicon wafer. A second silicon wafer consisting of the pressure sensitive diaphragms can then be bonded to the wafer containing the Bragg gratings. This structure then forms a hybrid two-dimensional array. Such a device will have many environmental limitations such as temperature but will provide an useful platform for the development of multiplexed readout techniques and the determination of environmental effects of specific applications. These fiber grating structures will use a second order grating scheme.

Figure 6 shows a conceptual sketch of a monolithic MOEMS pressure sensor array. This array utilizes a single fiber input and output to provide simultaneous output from each sensor in the array. Figure 6 shows an array of pressure sensing Si diaphragms formed on one wafer and a silicon-based optical waveguide interrogation network formed on the other. Optical interrogation of each individual element in the array is accomplished by directing light having multiple discrete wavelengths along the optical channel waveguide and using gratings, each tuned to a particular wavelength, to diffract light up to particular sensors. One unique aspect of our approach is the utilization of second order Bragg gratings for directing the light beam perpendicular to the surface. Although first order fiber and waveguide gratings have been extensively investigated [16], the use of second order gratings to couple light into and out of fibers and waveguides perpendicular to the waveguide axis has not yet been utilized.

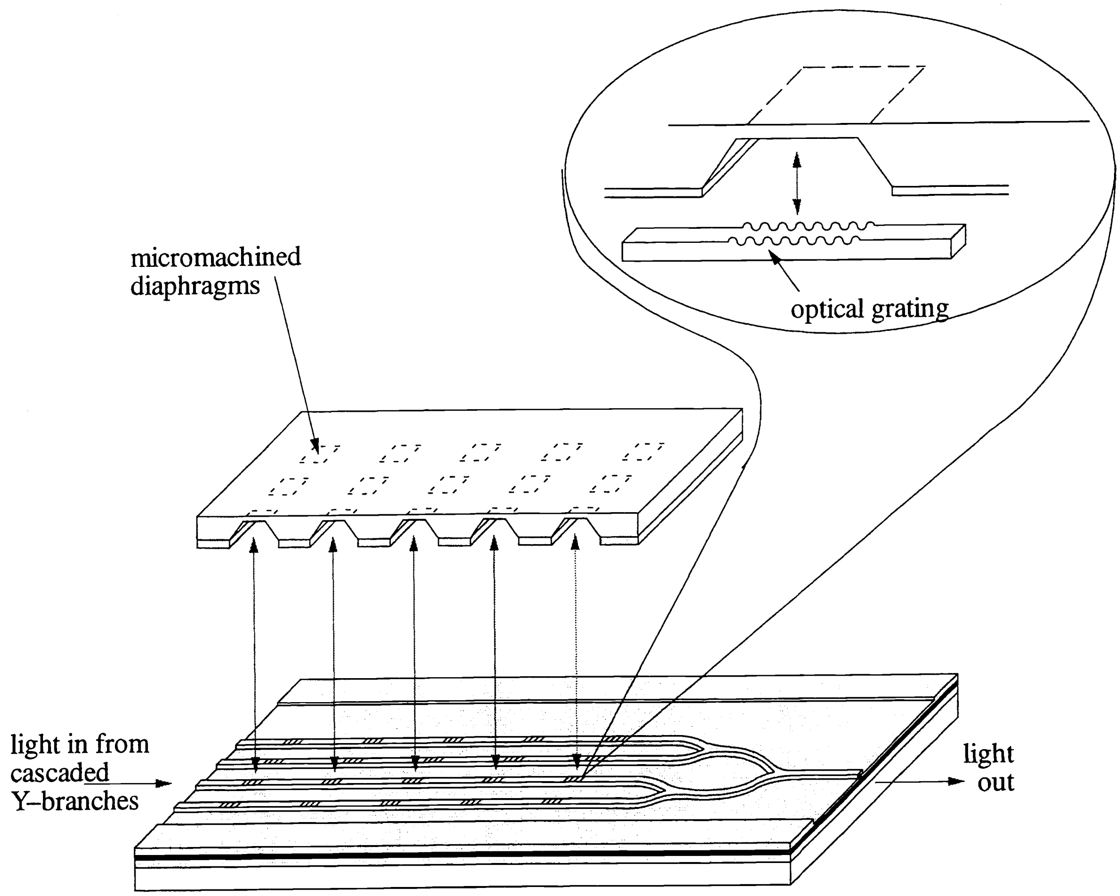

Figure 6. Micromachined diaphragms for use as pressure sensors optically interrogated by waveguide channels with grating structures to address each individual diaphragm with a different wavelength.

The concept of wavelength division multiplexing (WDM) is illustrated in Fig. 6 where light in channel waveguides is combined through cascaded y-junctions, as shown on the output, to comprise a single input and single output beam. When the wafers are complete, they would be aligned and electrostatically bonded so as to seal the cavities formed by the gratings and the diaphragms. For the pressure sensor array shown in Fig. 6, diaphragm deflection is detected interferometrically with the diaphragm surface and the grating surface acting as Fabry-Perot reflectors. Multiplexing using light and WDM information technology would significantly simplify system complexity required to interrogate an array of MEMS sensors. For MEMS sensor arrays operating in this manner, the sensor itself may be placed in the harsh environment whereas the electro-optic readout circuit may be placed in a remote and protected environment without a weight penalty.

4. SUMMARY

Pressure sensor arrays utilizing MEMS technology for fabrication of the sensing element and interrogation by fiber optics are described. We have demonstrated that these optically interrogated MEMS devices had excellent static and dynamic response characteristics for use as instrumentation in propulsion applications. Surface roughness proved to be an initial problem in the fabrication of arrays since the responsivity and range of the sensor are extremely sensitive to the diaphragm thickness. The etching process was then modified to obtain a smooth and uniform surface finish. Testing of arrays fabricated using the new process are currently in progress.

5. REFERENCES

1. B. Culshaw, G. W. Day, A. D. Kersey, and Y. Ohtsuka, editors, Special Issue on Optical Fiber Sensors, J. Lightwave Tech., vol. 13, July, 1995.
2. G. Beheim, K. Fritsch, and R. Poorman, "Fiber-linked Interferometric Pressure Sensor," Rev. Sci. Instrum. vol. 58, pp. 1655-1659 (1987).
3. R.A. Wolthuis, G.L. Mitchell, E. Saaski, J.C. Hartl, and M.A. Afromowitz, "Development of Medical Pressure and Temperature Sensors Employing Optical Spectrum Modulation," IEEE Transactions on Biomedical Engineering vol. 38, pp. 974-980 (1991).
4. Y. Kim and D. P. Neikirk, "Micromachined Fabry-Perot Cavity Pressure Transducer," IEEE Photonics Technology Letters, vol. 12, pp. 1471-1473 (1995).
5. G. Beheim and D.J. Anthan, "Fiber-Optic Photoelastic Pressure Sensor with Fiber-Loss Compensation," Opt. Lett. vol. 12, pp. 220-222 (1987).
6. D. Angelidis and P. Parsons, "Optical Micromachined Pressure Sensor for Aerospace Applications," Opt. Eng. vol. 31, pp. 1638-1641 (1992).
7. H. Unzeitig and H. Bartelt, "All-Optical Pressure Sensor with Temperature Compensation on Resonant PECVD Silicon Nitride Microstructures," Electronics Lett. vol. 28, pp. 400-402 (1992).
8. R. A. Atkins, J. H. Gardner, W. N. Gibler, C. E. Lee, M. D. Oakland, M. O. Spears, V. P. Swenson, H. F. Taylor, J. J. McCoy, and G. Beshouri "Fiber-Optic Pressure Sensors for Internal Combustion Engines," *Applied Optics*, **33 (7),** pp.1315-1320, March 1994.
9. J. Castracane and L. P. Chow, "Optical Multichannel Transducer Array for Wind Tunnel Applications, Optical Engineering, vol. 35, pp. 2627-2633 (1996).
10. M. Komachiya, H. Sônobe, T. Fumino, T. Sakaguchi, K. Kawakami, S. Wantanabe, and T. Sasayama, "Knocking Detection of a Gasoline Engine by Utilizing an Optical Fiber with Specific Refractive-Index Composition, Applied Optics, vol. 37, pp. 1152-1158 (1998).
11. M. Ohkawa, M. Izutsu, and T. Sueta, "Integrated Optic Pressure Sensor on Silicon Substrate," Appl. Opt. vol. 28, pp. 5153-5157 (1989).
12. G.N. De Brabander, J.T. Boyd, and Glenn Beheim, "Integrated Optical Ring Resonator with Micromechanical Diaphragm for Pressure Sensing," IEEE Photonics Technology Letters vol. 6, pp. 671-673 (1994).
13. A. Vadekar, A. Nathan, and W. P. Huang, "Analysis and Design of an Integrated Silicon ARROW Mach-Zehnder Micromechanical Interferometer", J. Lightwave Technol. vol. 12, pp. 157-162 (1994).
14. K. Fischer, J. Müller, R. Hoffmann, F. Wasse, and D. Salle, "Elastooptical Properties of SiON Layers in an Integrated Optical Interferometer Used as a Pressure Sensor," J. Lightwave Technol. vol. 12, pp. 163-169 (1994).
15. G. N. De Brabander, G. Beheim, and J. T. Boyd, "Integrated Optical Micromachined Pressure Sensor with Spectrally Encoded Output and Temperature Compensation," Applied Optics, vol. 37, pp. 3264-3267 (1998).
16. Paper 4178-39.
17. K. O. Hill and G. Meltz, "Fiber Bragg Grating Technology Fundamentals and Overview," J. Lightwave Tech. **15**, pp. 1263-1276, 1997.